

Received December 4, 2021, accepted December 13, 2021, date of publication December 23, 2021, date of current version January 5, 2022.

Digital Object Identifier 10.1109/ACCESS.2021.3138148

# Force Feedback Design of Operation Levers Considering the Characteristics of Human Force Perception to Improve Hydraulic Excavator Operability

RYOTA SEKIZUKA<sup>1</sup>, MASARU ITO<sup>2</sup>, CHIAKI RAIMA<sup>3</sup>, SEIJI SAIKI<sup>4</sup>,  
YOICHIRO YAMAZAKI<sup>4</sup>, AND YUICHI KURITA<sup>2</sup>, (Member, IEEE)

<sup>1</sup>Graduate School of Engineering, Hiroshima University, Hiroshima 739-8527, Japan

<sup>2</sup>Graduate School of Advanced Science and Engineering, Hiroshima University, Hiroshima 739-8527, Japan

<sup>3</sup>Digital Manufacturing Education and Research Center, Hiroshima University, Hiroshima 739-8527, Japan

<sup>4</sup>Kobelco Construction Machinery Company Ltd., Tokyo 141-8626, Japan

Corresponding author: Ryota Sekizuka (ryotasekizuka@hiroshima-u.ac.jp)

This work was supported by the Cooperative Research Project of Hiroshima University-KOBELCO Dream-Driven Research Center.

This work involved human subjects or animals in its research. Approval of all ethical and experimental procedures and protocols was granted by Hiroshima University-KOBELCO Dream-Driven Research Center.

**ABSTRACT** Appropriate reaction force design is essential to improve the lever operability of a hydraulic excavator that is difficult to operate. However, the force characteristics a human perceives when operating these levers are unknown. It is unclear whether the reaction force characteristics of the conventional lever are optimum for humans. Thus, this study aims to clarify the perceived force characteristics during the lever operation and verify the effectiveness of the lever reaction force design. In this study, a perceived force prediction method was proposed based on a musculoskeletal simulation for the lever operation. Also, it was confirmed that the perceived force could be estimated within a 7.8%–14.3% root mean square error. Furthermore, we developed the lever with the reaction force characteristics in which the perceived force varied linearly with the lever angle and confirmed that the proposed lever significantly improved operability when performing the leveling task with the excavator.

**INDEX TERMS** Sense of force, muscle activity, user interface, hydraulic excavator.

## I. INTRODUCTION

In construction fields, the number of industrial workers continuously decreases and productivity improvement has become a problem. Enhancing the work efficiency of a hydraulic excavator, which is a typical construction machine, is necessary for productivity improvement. The excavator is operated using two levers located at the left and right sides of the operator's seat. Fig. 1 shows the operation pattern of an excavator based on the ISO standard (ISO 10968:2020). To operate the excavator efficiently, the operator needs advanced skills. Sekizuka *et al.* developed a system aimed to increase the efficiency of operational training for the excavator and constructed evaluation indices for the operation

skills [1], [2]. This system easily enables training and is realized using a remote-controlled excavator and virtual reality technology.

Furthermore, it is essential to improve the excavator's operability. The feedback design of the operational interface of a tool or machine is directly linked to its operability. Conventional studies have shown that appropriate feedback design using graphics, sound, and vibration improves operability [3]–[5]. Ito *et al.* upgraded the operability of a teleoperated excavator by presenting the machine instability during excavation with visual information [6], [7]. The reaction force design of the operator interface also increases operability. Various studies have been conducted on force feedback devices to improve the operability of construction machinery by compensating for the lack of information when operating the excavator [8]–[10]. Some recent studies have

The associate editor coordinating the review of this manuscript and approving it for publication was Yongjie Li.

logically dealt with the force feedback control to present stable forces under the influence of external factors [11]–[13]. However, the force characteristics a human perceives when operating these levers are unknown. It is unclear whether the reaction force characteristics of the conventional lever without active force feedback and devices that present the machine's physical information in terms of force sensors are optimal for humans.

The operability of a vehicle's steering wheel changes when the reaction force characteristics vary. Takemura *et al.* reported that the subjective perceptual force obtained by psychophysical experiments correlated more with the steering wheel operability than the quantitative physical force measured by sensors [14]. Jones reported that the perceived force is affected by the physical characteristics of an object and the human psychophysical characteristics [15]. Furthermore, Takemura *et al.* reported that the perceptual force bias was affected by differences in posture while steering a vehicle [16]. McCloskey *et al.* revealed that the magnitude of effort is strongly correlated with the judgment of force and heaviness [17]. Cafarelli and Bigland-Ritchie discovered that the muscle activity could be used to estimate the effort [18]. Morree *et al.* provided neurophysiological evidence of the correlation between muscle activity and effort sensing [19]. These studies propose that the sense of effort can be predicted by estimating the muscle activity intensity. Kishishita *et al.* constructed a perceived force prediction model for steering operations by estimating the muscle activity based on posture, external force, and a three-dimensional (3D) musculoskeletal model [20]. They also explained the postural bias in the perception of the steering reaction force [21]. Thus, these previous studies advocate that the appropriate design of the perceived force can also enhance the operability of operational interfaces other than the steering wheel.

Our study aims to clarify the perceived force characteristics during the lever operation and verify the effectiveness of the lever reaction force design. Based on a musculoskeletal simulation, a perceived force prediction method is proposed for the lever operation. Moreover, the lever is adopted such that the perceived force varies linearly with the lever angle and verifies the effect of the proposed lever reaction force on the operability when performing the leveling task with the excavator. The problems dealt with in this study and their proposed solutions are presented below.

- 1) The force characteristics a human perceives when operating the lever are unknown, and no reaction force design method optimized for human senses has been proposed. We proposed a method for predicting the perceived force during the lever operation based on the muscle activity estimation by a musculoskeletal simulation.
- 2) It may be possible to improve the hydraulic excavator's operability by optimizing the lever reaction force for human force perception characteristics. The lever is developed such that the perceived force varies linearly

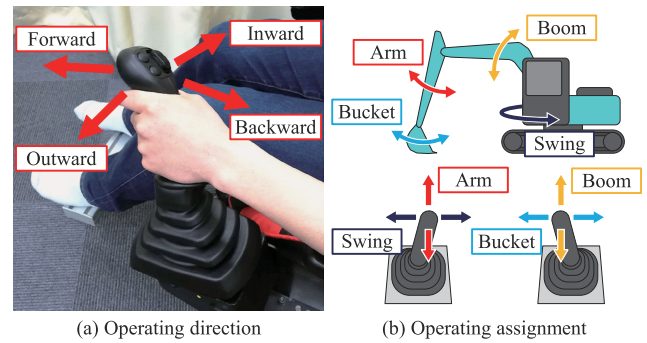


FIGURE 1. Conventional lever of a hydraulic excavator.

with the lever angle. Furthermore, we confirmed that the proposed reaction force characteristics improve the operability when performing the leveling task with the excavator. This finding suggests the superior effectiveness of considering the humanly perceived force than the physical force in the lever reaction force design.

The rest of this paper is organized as follows: Section II describes the construction of a perceived force prediction model for the lever operation. Next, Section III describes the verification of the designed lever's operability. Furthermore, Section IV discusses the results, and Section V concludes the study and presents future works.

## II. CONSTRUCTION OF PERCEIVED FORCE PREDICTION MODEL DURING LEVER OPERATION

### A. METHODOLOGY

In this study, a perceived force prediction model was constructed for the lever operation following the perceived force prediction method for the steering operation of a car, as proposed by Kishishita *et al.* [20]. Their estimation method is explained below. The perceived force when a reaction force is applied while holding the steering wheel is measured. The relationship between the applied force  $F_a$  and the perceived force  $F_p$  follows the Weber–Fechner law [22] and is approximated by the following equation:

$$F_p = a_0 \log F_a + b_0, \quad (1)$$

where  $a_0$  and  $b_0$  are coefficients when the steering angle is  $0^\circ$ . Here, the force perception-change ratio  $P$  is defined as follows:

$$P = \frac{F_p}{F_a} = \frac{a_0 \log F_a + b_0}{F_a}. \quad (2)$$

Here,  $P$  is determined uniquely using  $F_a$ . However, Takemura *et al.* reported that the perceived force changes depending on the body posture [16]. As described in the Introduction, a human judges the force based on the sense of effort [17]. The applied muscle varies according to posture, even when the hand outputs the force in the same direction and with identical magnitudes. Therefore, the sense of effort also changes when the posture varies. Cafarelli

and Bigland-Ritchie revealed that the muscle activity could be used to estimate the effort [18]. This fact suggests that describing the change in the perceived force depending on the posture can be actualized by expressing the force perception-change ratio using the muscle activity instead of the applied force. Kishishita *et al.* explained the force perception-change ratio using the muscle activity estimated by a 3D musculoskeletal simulation. They confirmed the linear relationship between the applied force  $F_a$  and muscle activity  $\alpha$  in the steering posture.  $\alpha$  is expressed by the following equation:

$$\alpha = k_j F_a + m_j, \quad (3)$$

where  $k_j$  and  $m_j$  are coefficients when the steering angle is  $j$ . (3) expresses the relationship between  $F_a$  and  $\alpha$  when the reaction force is applied while the steering angle is maintained at  $j$ .  $k_j$  and  $m_j$  are determined according to the posture in which the muscle activity is estimated because they change depending on the steering angle  $j$ . Furthermore, (3) shows that the postural effect on the muscle activity varies according to the steering angle and correlates with the human sense of force. The following equation is obtained by rearranging (3):

$$F_a = \frac{\alpha - m_j}{k_j}. \quad (4)$$

Then, the following equation is obtained by substituting (4) into (2):

$$P = \frac{F_p}{F_a} = \frac{k_j \left( a_0 \log \left( \frac{\alpha - m_j}{k_j} \right) + b_0 \right)}{\alpha - m_j}. \quad (5)$$

This equation demonstrates that the force perception-change ratio can be expressed as a function of the muscle activity based on the posture when the steering angle is  $j$ . The muscle activity can be obtained via optimization calculations using a musculoskeletal model with the posture and external force as inputs. Thus,  $P$  for a particular posture can be computed from the representative value of  $\alpha$ . Finally,  $F_p$  is given as a function of  $F_a$  by the following equation:

$$F_p = P \cdot F_a. \quad (6)$$

In this study, we constructed a perceived force prediction model for the lever following the above method. However, it was unconfirmed whether (1) and (3) are satisfied during the lever operation. Therefore, we investigated the perceived force and muscle activity characteristics for the applied force during the lever operation.

### B. MUSCLE ACTIVITY ESTIMATION BY MUSCULOSKELETAL SIMULATION

In this study, we estimated the muscle activity using OpenSim, an open-source software for biomechanical modeling, simulation, and analysis [23]. The 3D musculoskeletal model was developed based on the previously reported body model [24]. Moreover, the muscle force was calculated using

the muscle contraction model based on the Hill-type muscle model with elastic and contractile components proposed by Thelen [25]. The maximum isometric force  $F^M$ , optimal muscle-fiber length  $l^M$ , and pennation angle of the muscles were determined based on the parameters reported by Holzbaur *et al.* [26]. The muscle activity was obtained from the motion and external force data via optimization computations in OpenSim. First, the joint angle and torque were estimated by inverse kinematics and inverse dynamics calculations from the external force and marker position data measured using the motion capture system. Then, the muscle force that balances the joint torque was determined by optimizing the muscle activity. Here the muscle activity of the  $m$ -th muscle satisfies the following equation:

$$\sum_{m=1}^n (\alpha_m F_m^0) r_{m,j} = \tau_j, \quad (7)$$

where  $F_m^0$  is the maximum isometric force,  $\tau_j$  is the joint torque of the  $j$ -th joint, and  $r_{m,j}$  is the moment arm parameter.  $\alpha$  is a continuous variable bounded by  $\alpha_m (0 \leq \alpha_m \leq 1)$ ; it can be viewed as the controls to the musculoskeletal system [23]. By using the relationship between the motor unit firing rate and muscle activity, the muscle activity (muscle excitation) is increased by increasing the motor unit firing rate [27]. The moment arm parameters were determined using the muscle length of the  $m$ -th muscle  $l_m$  and joint angle of the  $j$ -th joint  $\theta_j$  [28], [29]:

$$r_{m,j} = \frac{dl_m}{d\theta_j}. \quad (8)$$

The relationship between the muscle force  $F_m$  and the muscle activity  $\alpha_m$  are given as follows:

$$F_m = \alpha_m F_m^0 \bar{f}_l(\bar{l}_m) + F_m^0 \bar{F}^{PE}(\bar{l}_m), \quad (9)$$

where  $\bar{l}_m$  is the normalized fiber length,  $\bar{f}_l(\bar{l}_m)$  is the normalized active force-length relationship, and  $\bar{F}^{PE}(\bar{l}_m)$  is the normalized passive force-length relationship; for this study,  $\bar{f}_l(\bar{l}_m)$  and  $\bar{F}^{PE}(\bar{l}_m)$  were obtained from a previous study [25].

### C. PERCEIVED FORCE CHARACTERISTICS FOR APPLIED FORCE

When the applied force was applied in the posture of holding the lever at the neutral position, the perceived force was measured to investigate the perceived force characteristics for the applied force in the lever operation. Fig. 2 shows the force presentation lever used in the experiment. This equipment has three components: a commercially available force feedback steering controller (Thrustmaster, T500RS), a grip part of the lever of an excavator, and a 3D printed part for attaching the grip to the steering shaft. The operation direction was switched by rotating the mounting direction of the grip 90° and rotating the sitting orientation with respect to the equipment 90° in the opposite direction. The game engine Unity was used to control the equipment's



FIGURE 2. Force presentation lever.

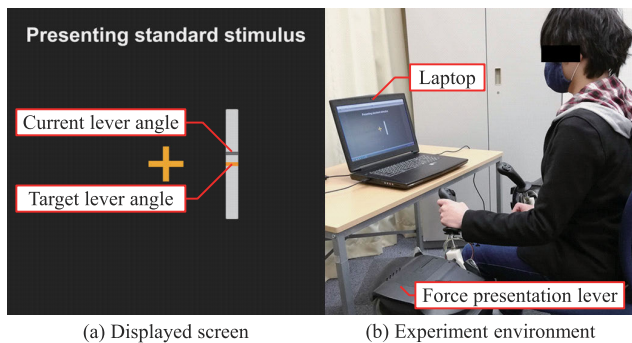


FIGURE 3. Measurement experiment of perceived force characteristics for the applied force. The image shows the subject with force applied while looking at the lever angle gauge displayed on the laptop. Informed consent was obtained from the individual for publishing this image.

applied force and perform the experiment. It was confirmed in advance that the equipment accurately outputs the force using the force sensor. Fig. 3 shows an image taken while measuring the perceived force characteristics for the applied force. The subjectively perceived force was measured using the magnitude estimation method [30]. The experimental procedure is as follows:

- 1) The subjects sit on the seat and hold the lever at the neutral position with their left hand. Afterward, a standard stimulus is given through the lever. The subjects hold the lever stationarily and memorize the standard stimulus.
- 2) Next, a comparison stimulus is given through the lever. Subsequently, the subjects report the magnification of the comparison stimulus relative to the standard stimulus.
- 3) The standard stimulus is 9 N, and the comparison stimuli range from 6 to 13 N with a 1-N increment. The comparison stimuli are presented at random, and steps 1) and 2) are repeated until each comparison stimulus is presented five times.

The above experimental tasks were conducted in four directions following the operation directions of the lever:

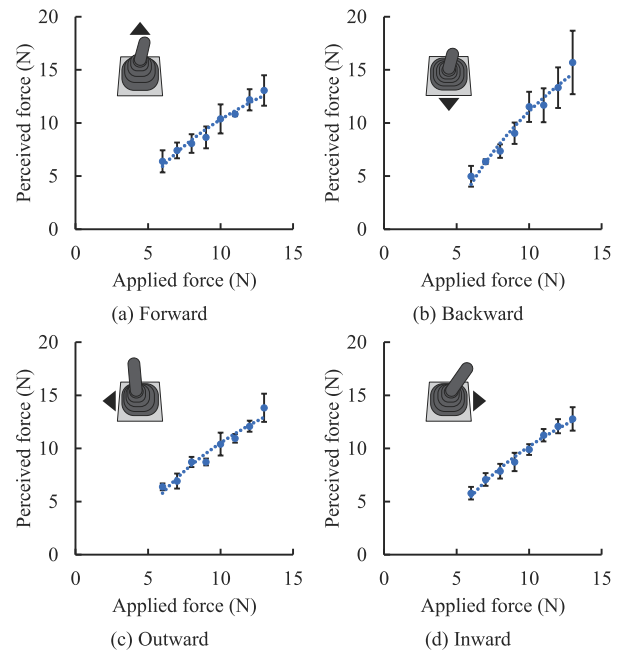


FIGURE 4. Perceived force characteristics for the applied force in each postural direction when the lever angle is 0°.

TABLE 1. Coefficients  $a_0$  and  $b_0$ , and the coefficients of determination  $R^2$ .

Direction	$a_0$	$b_0$	$R^2$
Forward	8.63	-9.54	0.965
Backward	13.40	-19.90	0.964
Outward	9.13	-10.50	0.953
Inward	9.21	-11.00	0.985

forward, backward, outward, and inward. The applied force was gradually increased for 4 s and afterward for 5 s more with a fixed force to avoid habituation error [31]. Three male subjects (average age:  $22.7 \pm 0.5$  years) participated in the experiment. Informed consent was obtained from the subjects, and their health conditions were verbally enquired. The subjects practiced the experimental task for about 5 min before the experiment.

Fig. 4 shows the perceived force characteristics with respect to the applied force for each operating direction. Here, the applied force acts opposite to the operation direction. The error bar represents the standard deviation of the perceived force of all subjects, and the dotted line represents the approximate curve. These results show that the perceived force is proportional to the logarithm of the applied force. The characteristics shown in this figure indicate that the relationship between the applied and perceived forces follows the Weber–Fechner law [22] and that (1) is satisfied even in the lever operation. The slope  $a_0$  and intercept  $b_0$  of the following equation that replaced (1) were calculated by the least-squares method from the measured perceived force for each applied force:

$$F_p = a_0 F'_a + b_0, \quad (10)$$



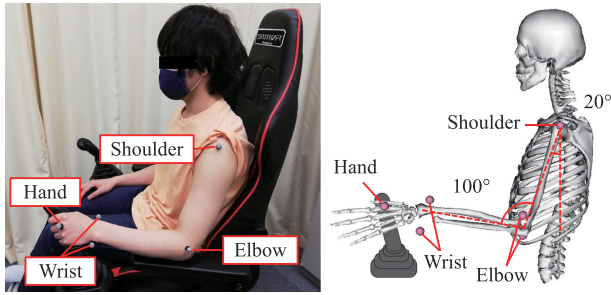


**FIGURE 5. Motion-capturing system and model postural conditions. Informed consent was obtained from the individual for publishing this image.**

where

$$F'_a = \log F_a. \quad (11)$$

The coefficient of determination  $R^2$  was calculated employing the following equation:

$$R^2 = 1 - \frac{\sum_{i=1}^n (y_i - \hat{y}_i)^2}{\sum_{i=1}^n (y_i - \bar{y})^2}. \quad (12)$$

Here,  $y_i$  is the  $i$ -th measured value,  $\bar{y}$  is the average value of the measured values, and  $\hat{y}_i$  is the  $i$ -th calculated value using the regression equation. Table 1 lists the coefficients  $a_0$  and  $b_0$ , and the coefficient of determination  $R^2$ .

#### D. MUSCLE ACTIVITY CHARACTERISTICS FOR THE APPLIED FORCE

When the force was applied in the posture of holding the lever at a certain angle, the muscle activity was estimated to investigate the muscle activity characteristics for the applied force during the lever operation. The muscle activity was estimated using OpenSim, an open-source software system for biomechanical modeling, simulation, and analysis [23]. Moreover, the stationary postures were obtained when holding the lever with the left hand at  $0^\circ$ – $25^\circ$  forward and backward and  $0^\circ$ – $20^\circ$  outward and inward with an interval of  $2.5^\circ$ . The postural data were obtained using seven motion capture cameras (Acuity Inc., OptiTrack PrimeX 13 W) installed around the subject. Fig. 5 shows the posture when holding the lever at the neutral and mounting positions of the motion capture markers. A force ranging from 0 to 12 N with a 2-N interval was directly applied to the capitate bone at the wrist because the muscles from the wrist to the fingertip were not considered. Herein, the average muscle activity was defined for the following muscles, which were especially active for each operational direction.

- Forward direction: the anterior head of the deltoid (DELTA1), medial head of the deltoid (DELTA2), infraspinatus (INFSP), and long head of the biceps brachii (BIClong)
- Backward direction: the posterior head of the deltoid (DELTA3), subscapularis (SUBSC), teres major (TMAJ), and long head of the triceps brachii (TRIlong)

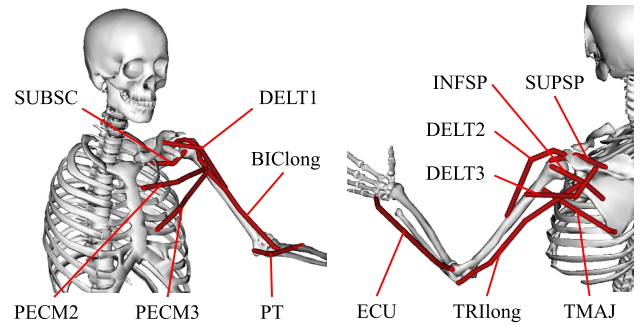


**FIGURE 6. Muscles applied to estimate muscle activity.**

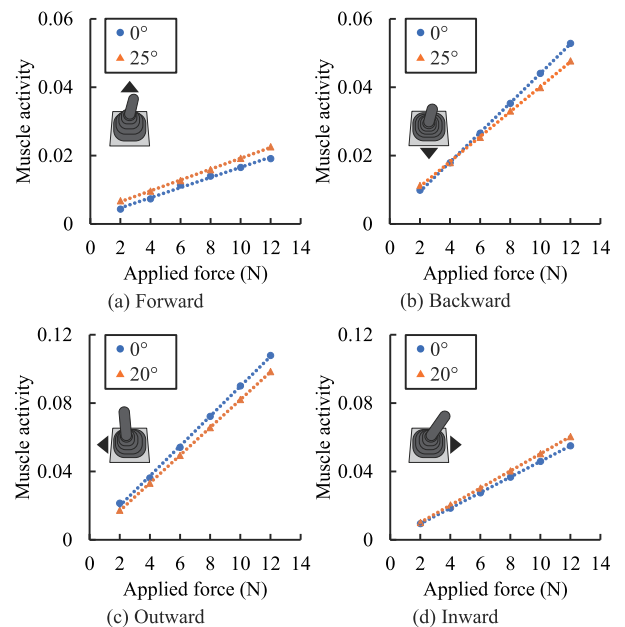


**FIGURE 7. Representative estimation results of activities of muscles that are actively involved when holding the lever. Circles and triangles indicate the results for  $0^\circ$  and the maximum lever angle in each operation direction, respectively.**

- Outward direction: the posterior head of the deltoid (DELTA3), supraspinatus (SUPSP), infraspinatus (INFSP), long head of the triceps brachii (TRIlong), and extensor carpi ulnaris (ECU)
- Inward direction: the subscapularis (SUBSC), teres major (TMAJ), sternocostal head of the pectoralis major (PECM2), abdominal head of the pectoralis major (PECM3), and pronator teres (PT)

Fig. 6 shows the muscles in the musculoskeletal model in OpenSim.

Fig. 7 shows an example of the muscle activity characteristics with respect to the applied force for each operating direction. The circles indicate the result at  $0^\circ$  of the lever angle, whereas the triangles indicate the result at the maximum lever angle in each operation direction. The dotted lines indicate approximate lines. These results suggest that the muscle activity is proportional to the applied force and that (3) is satisfied even during the lever operation. The

TABLE 2. Coefficients  $k_j$  and  $m_j$ , and the coefficient of determination  $R^2$ .

$j$	Forward			Backward		
	$k_j$	$m_j$	$R^2$	$k_j$	$m_j$	$R^2$
0	0.00150	0.00159	0.992	0.00432	0.00088	1.000
2.5	0.00124	0.00317	1.000	0.00428	0.00096	1.000
5	0.00125	0.00343	1.000	0.00423	0.00132	1.000
7.5	0.00127	0.00315	1.000	0.00402	0.00298	0.999
10	0.00156	0.00218	0.988	0.00402	0.00262	0.999
12.5	0.00145	0.00246	0.981	0.00401	0.00262	0.999
15	0.00133	0.00350	1.000	0.00392	0.00302	0.999
17.5	0.00140	0.00330	0.999	0.00387	0.00320	1.000
20	0.00145	0.00344	0.999	0.00381	0.00338	1.000
22.5	0.00152	0.00347	0.999	0.00376	0.00348	0.999
25	0.00159	0.00337	0.999	0.00365	0.00366	1.000

$j$	Outward			Inward		
	$k_j$	$m_j$	$R^2$	$k_j$	$m_j$	$R^2$
0	0.00874	0.00246	0.999	0.00455	0.00033	1.000
2.5	0.00876	0.00088	1.000	0.00463	0.00012	1.000
5	0.00860	0.00085	1.000	0.00464	0.00050	1.000
7.5	0.00854	0.00085	1.000	0.00474	0.00018	1.000
10	0.00846	0.00083	1.000	0.00477	0.00020	1.000
12.5	0.00837	0.00082	1.000	0.00486	0.00023	1.000
15	0.00832	0.00082	1.000	0.00492	0.00022	1.000
17.5	0.00832	0.00084	1.000	0.00496	0.00021	1.000
20	0.00812	0.00084	1.000	0.00502	0.00021	1.000

slope  $k_j$  and intercept  $m_j$  of (3) were calculated using the least-squares method from the estimated value of the  $\alpha$  for each  $F_a$  value at the lever angle  $j$ .  $R^2$  was calculated using (12). Table 2 lists the coefficients  $k_j$  and  $m_j$ , and the coefficient of determination  $R^2$ .

E. PERCEIVED FORCE ESTIMATION DURING LEVER OPERATION

The muscle activity was calculated when a force of 6 N was applied at each lever angle using (3) and the coefficients listed in Table 2. Also, the force perception-change ratio was determined by substituting the muscle activity at each lever angle into (5) ( $j = 0$ ). Fig. 8 shows the muscle activity and the force perception-change ratio with respect to the lever angle. Evidently, the muscle activity and force perception-change ratio change slightly according to the posture even when the same force is applied. The perceived force can be calculated using the force perception-change ratio and (6). Fig. 9 shows the relationship between the calculated perceived force, lever angle, and applied force. Evidently, the perceived force increases logarithmically as the applied force increases. Furthermore, the posture-changing effect according to the lever angle on the perceived force is comparatively small. We calculated the estimated perceived force for each angle of the conventional lever using this model and compared it with the measured perceived force.

The perceived force was measured using the magnitude estimation method [30]. The experimental environment was the same as described in Section II-C and shown in Fig. 3. However, the excavator lever was used instead of the force presentation lever. The experimental procedure is as follows:

- 1) The subjects sit on the seat and hold the lever with their left hand. Then, the subjects operate the lever to the target angle while looking at the displayed gauge,

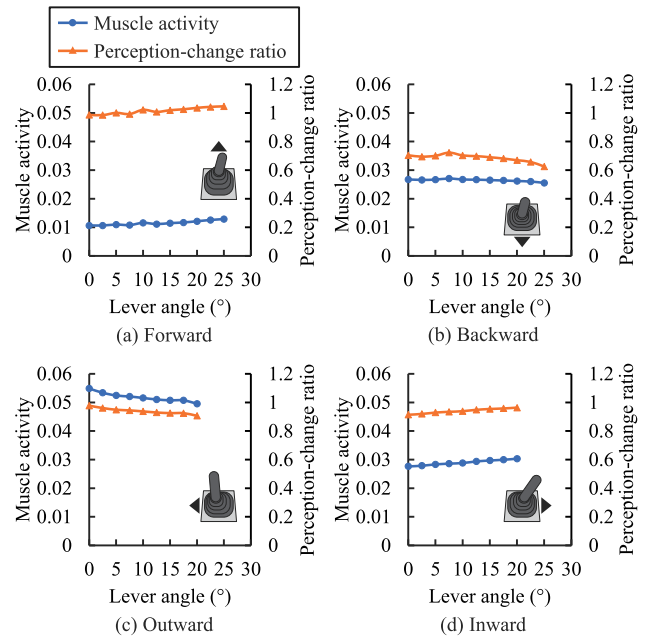


FIGURE 8. Muscle activity and force perception-change ratio with respect to lever angle (6-N force is applied).

which shows the present and target angles of the lever, and holds the lever stationarily at the target angle for 5 s. Also, the subjects memorize the magnitude of the perceived force at that time. The first target angle is set to a standard angle. The display position of the target angle on the gauge is always set to the center to prevent the subject from judging the target angle using the gauge as much as possible.

- 2) The target angle is changed to the comparison angle, and the subject operates the lever as in step 1). Afterward, the subject reports the magnification of the perceived force for the comparison angle relative to the perceived force for the standard angle.
- 3) The standard angle is 12° forward and backward and 10° outward and inward. The comparison angles range from 6° to 20° forward and backward and from 4° to 16° outward and inward with an interval of 2°. The comparison angles are randomly displayed, and steps 1) and 2) are repeated until each comparison angle is displayed five times.

The above tasks were performed forward, backward, outward, and inward. The subjects were the same three subjects who participated in the experiment described in Section II-C, and informed consent was obtained. The subjects practiced the experimental task for about 5 min before the experiment.

Fig. 10 shows the estimated and measured values of the perceived force for each lever angle. The circles indicate the estimated perceived force, the triangles indicate the measured perceived force, and the crosses indicate the reaction force of the lever. The root mean square percentage error (RMSPE) between the estimated and measured perceived force was determined to confirm the estimation accuracy. The cubic

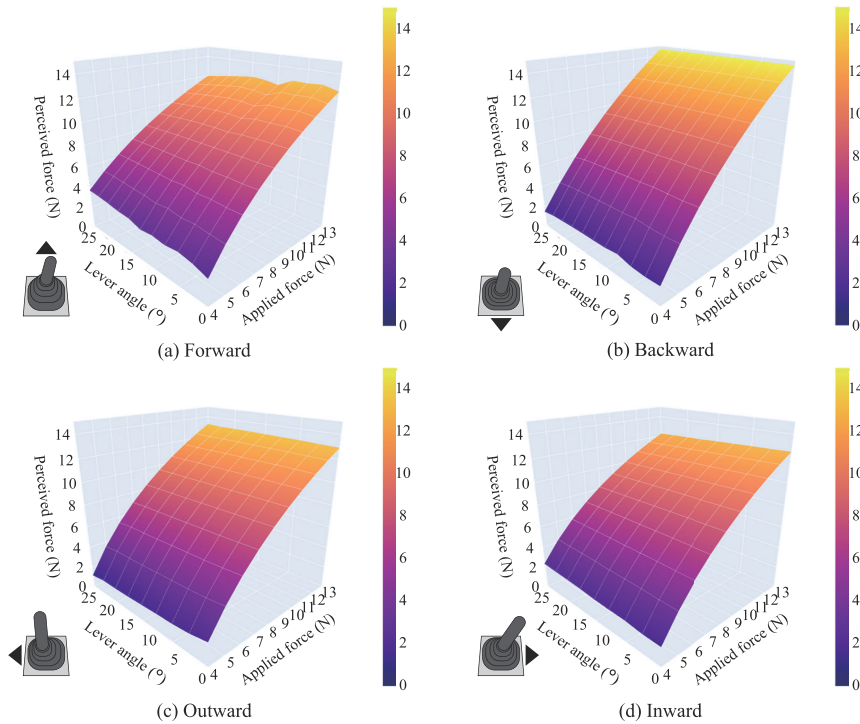


FIGURE 9. Predicted perceived force with respect to lever angle and applied force.

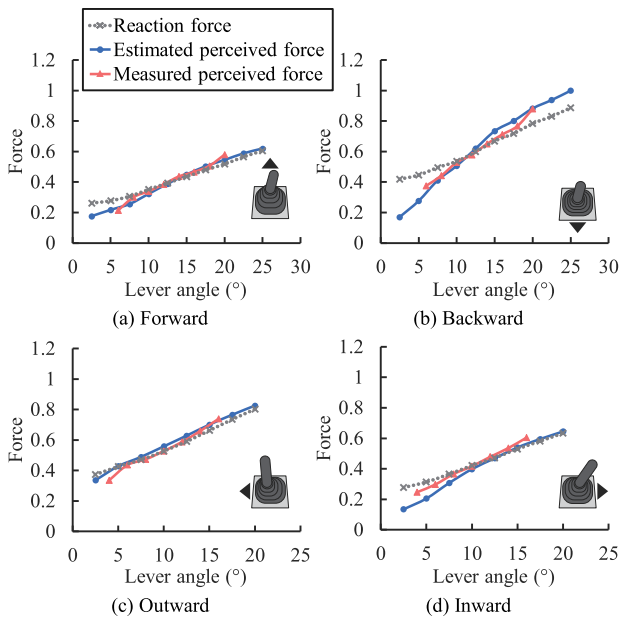


FIGURE 10. Estimated and measured perceived forces of conventional lever. Each value was normalized by the maximum value of the estimated perceived force in four directions.

spline interpolation was used for the estimated values because the ranges and intervals of the estimated and measured values differed due to the experimental environment variation. The following are the RMSPE values: 5.7% for 6°–20° forward, 6.0% for 6°–20° backward, 7.8% for 4°–16° outward, and 14.3% for 4°–16° inward.

### III. VERIFICATION OF LEVER REACTION FORCE DESIGN CONSIDERING FORCE PERCEPTION CHARACTERISTICS

#### A. DESIGN OF LEVER REACTION FORCE

The reaction force of the lever was designed considering the force perception characteristics using the constructed prediction model of the perceived force. Fig. 10 shows that the conventional force perception characteristics are nonlinear and asymmetric in all four directions: forward, backward, outward, and inward. These unreasonable and complicated characteristics may cause discomfort during the lever operation and make the excavator operation more difficult. Thus, we propose linear and symmetric reaction force characteristics in the forward, backward, outward, and inward directions. The reaction force characteristics were calculated numerically from the target perceived force using the constructed model, as described in Section II. Furthermore, the maximum value of the target perceived force equivalent was set to that of the conventional lever. Fig. 11 shows the proposed target perceived force and the calculated reaction force necessary to realize it. The circles and crosses indicate the proposed perceived and reaction forces, respectively.

#### B. OPERATING SIMULATOR OF HYDRAULIC EXCAVATOR USED FOR OPERABILITY EVALUATION

The operability of the proposed reaction force design was evaluated using the operating simulator of a hydraulic excavator (Fig. 12). This simulator is similar to the simulator used in the previous study [7] except for the lever, seat,

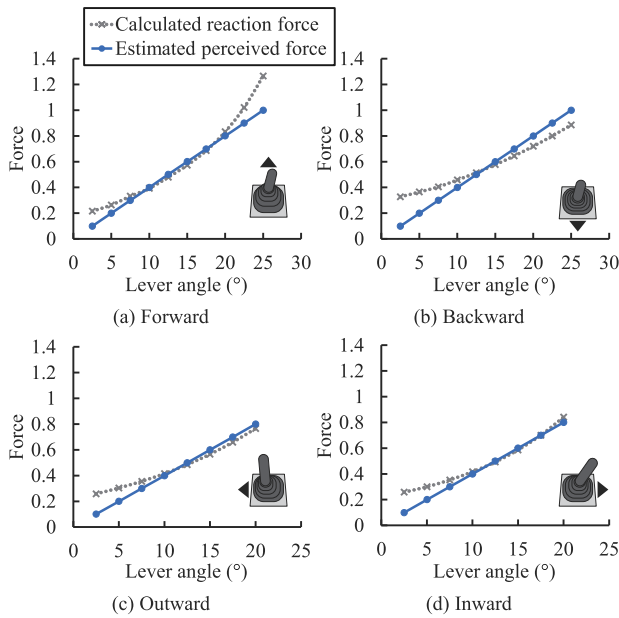


**FIGURE 11.** Proposed perceived and calculated reaction force characteristics. Each value was normalized by the maximum value of the perceived force in four directions.

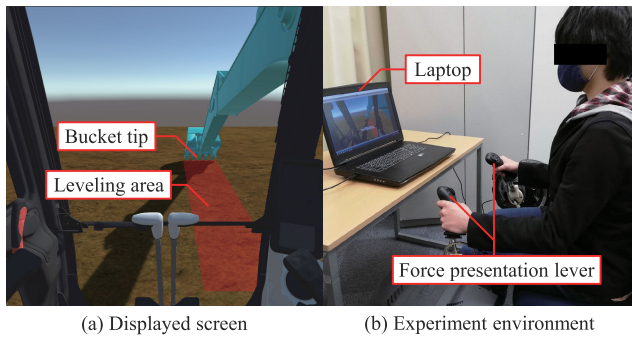


**FIGURE 12.** Operating simulator of a hydraulic excavator. The image shows the subject performing the leveling task. Informed consent was obtained from the individual for publishing this image.

and display. The simulator was built using the game engine Unity, and the excavator could be operated with the force presentation levers (Fig. 2). The system of each operated joint of the hydraulic excavator was approximated as the first-order lag system with the dead time in the simulator. The 3D model of the excavator was created based on the CAD data of the 13-ton hydraulic excavator manufactured by Kobelco Construction Machinery Co., Ltd. The cab view of the excavator in the simulator was displayed on the screen. It has been reported that the results were similar to those of the real excavator when evaluating the digging work [7].

We investigated the presence of the cab view displayed on the screen and system usability when using the simulator instead of a real excavator. The reaction force characteristics of the force presentation lever were those of the conventional lever of a hydraulic excavator. Four male subjects (average age:  $23.5 \pm 1.7$  years) who had experience operating a real

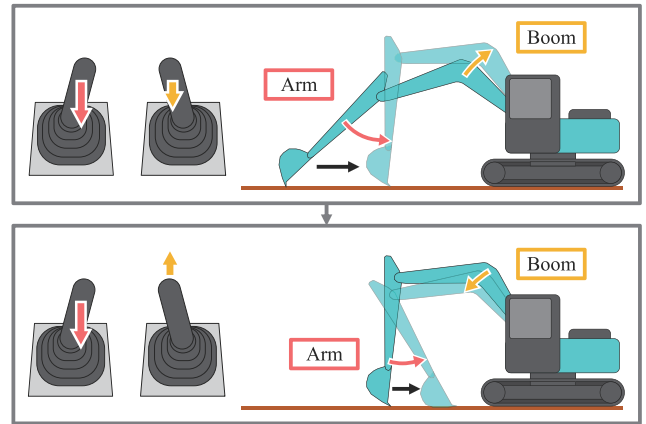


**FIGURE 13.** Lever operation during leveling task.

excavator participated in the experiment. Informed consent was obtained from the subjects, and their health conditions were verbally enquired. The subjects performed the leveling tasks by the simulator and answered the questionnaire. The leveling task entails moving the bucket tip parallel to the ground (Fig. 13). Herein, the bucket angle was fixed, and the leveling work was performed only by operating the boom and arm. The leveling task, which involved pulling and pushing, was repeated 10 times. The presence of the cab view displayed on the screen was evaluated using four items (“presence,” “powerfulness,” “comfortableness,” and “depth”) by referring to an evaluation questionnaire for the presence of a wide-field still image [32]. Each item was answered with a 7-point scale from 1 to 7, corresponding to “Bad,” “Poor,” “Fairly poor,” “Fair,” “Fairly good,” “Good,” and “Excellent.” The system usability was evaluated using the System Usability Scale (SUS) [33]; a 10-item questionnaire for measuring a system’s usability with a score ranging from 0 to 100.

Table 3 shows the mean scores for the presence of the cab view and system usability. Each number in parentheses represents the standard deviation. The mean scores of “presence” and “comfortableness” exceeded five points, corresponding to “Fairly good.” The mean score of “powerfulness” exceeded four points, corresponding to “Fair,” and that of “depth” was below four points. By performing the Student’s one-sample *t*-test for the SUS score, a significant difference from the test value of 68 (the standard average of SUS score) was confirmed. Although there was no room for improvement in the presence of the cab view, the system usability was high enough that the simulator could be used to evaluate the lever’s operability instead of the real excavator.

### C. EVALUATION EXPERIMENT

The operability of the excavator was evaluated using the simulator to verify the effectiveness of the proposed reaction force design. The leveling task, involving pulling and pushing, was repeated 10 times in the experiment. Fig. 12 shows a subject performing the leveling task. Seven male subjects



**TABLE 3.** Mean scores (standard deviation in parenthesis) for the presence of the cab view and system usability.

Item	Mean score (standard deviation)
Presence	5.00 (1.22)
Powerfulness	4.25 (0.83)
Comfortableness	5.50 (0.87)
Depth	3.75 (0.83)
SUS	80.00 (4.68)

(average age:  $23.1 \pm 1.4$  years) who had no excavator experience participated in the experiment. Informed consent was obtained from the subjects, and their health conditions were verbally enquired. Before the experiment, the subjects underwent one training session, in which the operating speed was controlled by reproducing the leveling operation performed by the expert on the simulator with the gauge of the lever operation amount assigned to the subjects. The leveling task was practiced 10 times by each of the inexperienced subjects. Three reaction forces were randomly applied for each subject: the proposed, conventional, and zero reaction forces. The conventional reaction force characteristics are the reaction force characteristics of the conventional hydraulic excavator's lever (Fig. 10). Herein, the operability of an excavator is considered from the following viewpoints: 1) how accurately the operators can operate, 2) how not tired they are during the operation, and 3) how much they can operate as they wish. The evaluation indices for operability are as follows.

- Mean bucket trajectory and dispersion of bucket trajectories: These indices were calculated using dynamic time warping (DTW) [34], a method for calculating the dissimilarity between two time-series data, and DTW barycenter averaging [35], a method for calculating the average time-series data.
- Time: The time required for one leveling task was considered. This index was used to confirm whether the operation time was controlled.
- Mean absolute error (MAE): The mean absolute distance between the bucket tip and ground during one leveling task was calculated using the following equation.

$$MAE = \frac{1}{N} \sum_{i=0}^N |y_i|, \quad (13)$$

where  $|y_i|$  is the absolute distance between the bucket tip and the ground, and  $N$  is the number of samples of data measured in one leveling task.

- Workload: The workload is the average score of six items in the Japanese version [36] of NASA-TLX [37]. The items were measured on a 101-point scale from 0 to 100.
- Sense of agency (SoA): The average score of 11 out of 21 items in the SoA scale for heavy machine operation [38], excluding items unrelated to the leveling task of the experiment, was considered. The items were measured on a 7-point scale from 1 to 7.

The questions for examining the workload and SoA are listed in Tables 4 and 5, respectively.

**TABLE 4.** Questions for examining the workload.

No.	Item
1	How much mental and perceptual activity was required?
2	How much physical activity was required?
3	How much time pressure did you feel due to the pace at which the tasks or task elements occurred?
4	How successful were you in performing the task?
5	How hard did you have to work to accomplish your level of performance?
6	How irritated, stressed, and annoyed versus content, relaxed, and complacent did you feel during the task?

**TABLE 5.** Questions for examining the sense of agency.

No.	Item
1	I operate the machine instinctively without thinking.
2	I operate the machine as if moving my arms and legs.
3	I can control and grasp the position of the machine's attachment or blade.
4	I feel the machine moves in correspondence to my lever operation.
5	I can operate according to the work process or goal I anticipated.
6	I can operate based on the machine's characteristic (inertia of the machine's movement, the machine's width, etc.)
7	I feel my operation is good.
8	I feel as if I could cause movement of the machine.
9	I feel as if I could control the movements of the machine.
10	The machine is obeying my will and I can make it move just like I want it.
11	I operate the machine carefully.

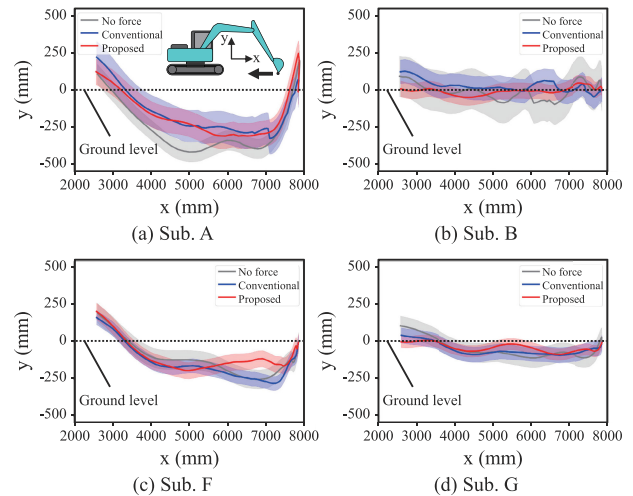


**FIGURE 14.** Mean bucket trajectory in leveling task for each subject (pulling direction).

Fig. 14 shows the mean bucket trajectory and dispersion of the trajectory during the leveling task (pulling direction) for subjects A, B, F, and G as an example. The solid gray lines indicate the mean trajectory with no reaction force, and the solid blue lines indicate the mean trajectory as per the conventional reaction force. Furthermore, the solid red lines indicate the mean trajectory as per the proposed reaction force. The semitransparent areas indicate the bucket trajectory dispersion. Also, the black dotted lines indicate the ground level. The results show that the trajectories achieved

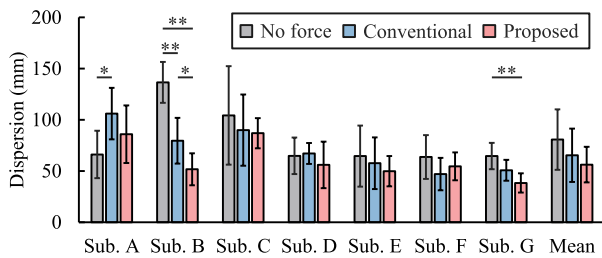


**FIGURE 15.** Dispersion of bucket trajectories in leveling task for each subject (pulling direction, \*:  $p < 0.05$ , \*\*:  $p < 0.01$ ).

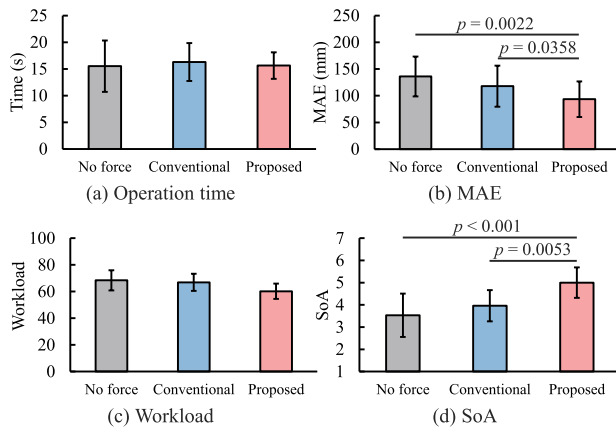


**FIGURE 16.** Evaluation results for each reaction force characteristics in the leveling task.

by applying the proposed reaction force are smooth curves and tend to be the closest to the ground. Fig. 15 shows the dispersion of the bucket trajectories in the pulling direction of the leveling task for each subject and the mean dispersion for all subjects. The asterisks on the graph indicate significant differences (\*:  $p < 0.05$ , \*\*:  $p < 0.01$ , one-way analysis of variance [ANOVA] followed by the Student's  $t$ -test with adjusted  $p$  values by the Holm method [39]). The dispersion for the proposed reaction force was the smallest though there was no significant difference between the three conditions in the mean dispersion of the trajectories of all subjects.

Fig. 16 shows the averages of the time, MAE, workload, and SoA for all the subjects. The error bar represents the standard deviation of the values for all subjects. The  $p$  values on the graph indicate significant differences at the 5% level (one-way ANOVA followed by the Student's  $t$ -test with adjusted  $p$  values by the Holm method [39]). There was no significant difference in the time between the three conditions because the operating speed was controlled in the experiment. It was confirmed that the MAE for the proposed reaction force was significantly less than that for the other. There was no significant difference in the workload between the three conditions, but the workload for the proposed reaction force was the least. Furthermore, the SoA for the proposed reaction force was significantly lower than that for the other. These results suggest that the linear and symmetric reaction force design improves the working accuracy and SoA.

#### IV. DISCUSSION

In this study, we conducted an experiment in which subjects answered their perceived force during the lever operation. We also constructed a model to predict the perceived force from the muscle activity estimated based on the posture and reaction force during the lever operation. This method has been proposed to estimate the perceived steering wheel operation force [20]. It has also been shown to be capable of explaining the force perception bias during the steering wheel operation [21]. We considered that this method could be applied to estimate the perceived force during the lever operation and designed the experiment for this study.

The perceived force differs depending on the operating direction, even for identical magnitudes of the lever reaction force (Fig. 4). Meanwhile, Fig. 9 shows that the perceived force is less affected by the lever angle in all operating directions. Fig. 7 indicates that muscle activity has the same tendency as the perceived force. These results are supported by the fact that the magnitude of effort is strongly correlated with the judgment of force, as reported by McCloskey *et al.* [17], and by the neurophysiological evidence that muscle activity and sense of effort are correlated, as reported by Morree *et al.* [19]. Fig. 10 shows the estimated and measured values of the perceived force for each lever angle. The perceived force can be estimated with RMSPE values of 5.7% and 6.0% in the range of  $6^\circ$ – $20^\circ$  forward and backward, respectively, and 7.8% and 14.3% in the range of  $4^\circ$ – $16^\circ$  outward and inward, respectively. This result indicates that the subjectively perceived force during the lever operation can be predicted computationally. When using conventional techniques, it is necessary to conduct an experiment in which the subjects report the perceived forces for all lever angles to conventionally obtain the force perception characteristics during the lever operation. Furthermore, the perceived force can be computationally estimated from musculoskeletal simulation without subject experimentation using the proposed method. The proposed method allows us to obtain the force perception quantity at a lower experimental cost than the conventional method. Fig. 11 shows the proposed perceived and calculated reaction forces. As mentioned above, the perceived force characteristics differ depending on the operating direction. The reaction force characteristics vary directionally when the force perception characteristics are identical in all directions. Furthermore, the relationship between the reaction and perceived forces can be roughly explained by the Weber–Fechner law [22], regardless of the lever angle because the effect of the lever angle on force the perception is small. Therefore, the calculated reaction force is approximately proportional to the exponential function of the lever angle. In this study, we hypothesized that the reaction force design in which the perceived force varies linearly with the lever angle improved the operability of the leveling operation of the excavator. Indeed, our results verify this hypothesis. Fig. 14 shows an example of the bucket trajectory. As per the proposed force

perception characteristics, the trajectory is the closest to the ground and is a smooth curve. The results in Fig. 16 indicate that the linear and symmetric reaction force design improves the working accuracy and SoA in the leveling operation. These results may be attributed to the proper design of the force perception characteristics of the lever. Consequently, this finding supports the study's hypothesis.

However, the perceived force estimation method used for the reaction force design in this study has some limitations. First, the proposed method does not consider individual differences, such as the operator's physique and operational proficiency. The perceived force was estimated in the fixed posture using a standard human musculoskeletal model. However, the parameters, such as bone length and origin of each muscle, differ per person, and the operating posture also changes depending on the physique. Since the method adopted in this study depends on the simulation accuracy of the muscle activity, if the human body model is hugely different from the operator's physique, the estimation accuracy of the perceived force may decrease. Moreover, we did not verify the effectiveness of the proposed reaction force characteristics for operators who are accustomed to the lever of the conventional reaction force characteristics. The skilled and nonskilled operators may operate the same lever in different postures and with varying usages of muscles. Muscle co-contraction controls the joint stiffness [40] and helps humans realize accurate movements [41], [42]. Osu *et al.* showed that co-contraction gradually decreases during the learning process of a new motor task [43]. This finding suggests that the skilled operator operates the lever with less muscle force. Since co-contraction is not considered in the musculoskeletal simulation used in the proposed method, the estimation accuracy of muscle activity may decrease, especially for operators who are unaccustomed to operating excavators. Using a musculoskeletal model suitable for the operator's physique and considering muscle co-contraction is essential for improving the estimation accuracy of muscle activity. Also, it is necessary to verify the effectiveness of the proposed perceived force characteristics for an operator who is sufficiently accustomed to the lever of the conventional perceived force characteristics. Second, only static musculoskeletal simulations were performed in this study. However, in reality, the lever operation involves dynamic postural changes. Mitchell *et al.* reported that dynamic exercises involve changes in muscle length and joint movement with rhythmic contractions, resulting in reduced intramuscular forces compared to those involved in static exercises [44]. Muscle activity characteristics differ depending on whether the movement is dynamic or static. Dynamic musculoskeletal simulations require sophisticated algorithms. Third, although the results of efferent signals, i.e., muscle activity, were used to estimate the force perception in this study, afferent signals from muscle spindles and peripheral skin receptors are also essential factors in determining a sense of force [45]–[47]. As described in Section I, muscle activity as a sense of effort can be

used to predict the sense of force. However, Phillips *et al.* proposed that the sense of force should be predicted based on the sense of effort and the afferent feedback from the periphery [48]. Monjo *et al.* proposed that humans do not perceive only efferent or afferent signals as a sense of effort; in fact, the sense of effort is perceived by changes in the balance of the two signals according to the experimental conditions [49]. The sense of force may be altered by the influence of afferent signals from peripheral skin receptors due to skin vibration and deformation in the case of a lever in the cab to which the engine vibration transmits, or a lever implemented with vibration feedback [50], [51] or skin deformation feedback [52]–[54]. Hence, it is essential to consider afferent signals from muscle spindles and peripheral skin receptors to improve the estimation accuracy of force perception. Fourth, the force perception in the combined operation of the longitudinal and lateral directions remains unverified. It may be difficult to perceive the reaction force in the longitudinal and lateral directions independently due to the duplication between the active muscles when operating the lever in these directions. Building a lever corresponding to two axes is necessary because the force presentation lever used in this study has only one axis. A lever reaction force design more suitable for determining the human force perception characteristics can be realized by solving these problems.

Moreover, in this study, only the simulator was used to verify the operability of the proposed reaction force lever, and it is uncertain whether the same results can be obtained in the real excavator. The verification using a real excavator will be included in future work.

## V. CONCLUSION

In this study, we proposed a lever reaction force design considering human force perception characteristics. We estimated the force perception characteristics in operating a lever of an excavator by muscle activity estimation using musculoskeletal simulation. The results showed that the perceived force in the lever operation could be computationally predicted. We evaluated the lever reaction force characteristics designed based on the clarified force perception characteristics. Furthermore, we confirmed that the reaction force design in which the force perception characteristics are linear and symmetric in each direction improved the operability of the excavator's leveling operation. In the future, we will estimate the perceived force considering the combined operation of the longitudinal and lateral directions of the lever and evaluate the operability in other tasks, such as excavation work. Furthermore, we will verify the operability of the proposed reaction force lever with a real excavator.

## REFERENCES

- [1] R. Sekizuka, K. Koiwai, S. Saiki, Y. Yamazaki, T. Tsuji, and Y. Kurita, "A virtual training system of a hydraulic excavator using a remote controlled excavator with augmented reality," in *Proc. IEEE/SICE Int. Symp. Syst. Integr. (SII)*, Dec. 2017, pp. 893–898.

- [2] R. Sekizuka, M. Ito, S. Saiki, Y. Yamazaki, and Y. Kurita, "Evaluation system for hydraulic excavator operation skill using remote controlled excavator and virtual reality," in *Proc. IEEE/RSS Int. Conf. Intell. Robots Syst. (IROS)*, Nov. 2019, pp. 3229–3234.
- [3] M. E. Altinsoy and S. Merchel, "Audiotactile feedback design for touch screens," in *Proc. Int. Conf. Haptic Interact. Design*. Berlin, Germany: Springer, 2009, pp. 136–144.
- [4] Y. Song, S. Guo, X. Yin, L. Zhang, H. Hirata, H. Ishihara, and T. Tamiya, "Performance evaluation of a robot-assisted catheter operating system with haptic feedback," *Biomed. Microdevices*, vol. 20, no. 2, pp. 1–16, Jun. 2018.
- [5] M. Haruna, M. Ogino, and T. Koike-Akino, "Proposal and evaluation of visual haptics for manipulation of remote machine system," *Frontiers Robot. AI*, vol. 7, Oct. 2020, Art. no. 529040.
- [6] M. Ito, C. Raima, S. Saiki, Y. Yamazaki, and Y. Kurita, "A study on machine instability feedback during digging operation in teleoperated excavators," in *Proc. 13th Int. Conf. Human Syst. Interact. (HSI)*, Jun. 2020, pp. 14–19.
- [7] M. Ito, C. Raima, S. Saiki, Y. Yamazaki, and Y. Kurita, "Effects of machine instability feedback on safety during digging operation in teleoperated excavators," *IEEE Access*, vol. 9, pp. 28987–28998, 2021.
- [8] Y.-J. Nam and M.-K. Park, "Virtual excavator simulator featuring HILS and haptic joysticks," *J. Mech. Sci. Technol.*, vol. 29, no. 1, pp. 397–407, Jan. 2015.
- [9] D. Q. Truong, B. N. M. Truong, N. T. Trung, S. A. Nahian, and K. K. Ahn, "Force reflecting joystick control for applications to bilateral teleoperation in construction machinery," *Int. J. Precis. Eng. Manuf.*, vol. 18, no. 3, pp. 301–315, Mar. 2017.
- [10] C. S. Meera, P. S. Sairam, V. Veeramalla, A. Kumar, and M. K. Gupta, "Design and analysis of new haptic joysticks for enhancing operational skills in excavator control," *J. Mech. Des.*, vol. 142, no. 12, Dec. 2020, Art. no. 121406.
- [11] Z. Chen, F. Huang, C. Yang, and B. Yao, "Adaptive fuzzy backstepping control for stable nonlinear bilateral teleoperation manipulators with enhanced transparency performance," *IEEE Trans. Ind. Electron.*, vol. 67, no. 1, pp. 746–756, Jan. 2020.
- [12] J. Guo, L. He, and S. Guo, "Study on force feedback control of the vascular interventional surgical robot based on fuzzy PID," in *Proc. IEEE Int. Conf. Mechatronics Automat. (ICMA)*, Oct. 2020, pp. 1710–1715.
- [13] A. Sayadi, A. Hooshier, and J. Dargahi, "Impedance matching approach for robust force feedback rendering with application in robot-assisted interventions," in *Proc. 8th Int. Conf. Control, Mechatronics Automat. (ICCA)*, Nov. 2020, pp. 18–22.
- [14] K. Takemura, N. Yamada, A. Kishi, K. Nishikawa, T. Nouzawa, Y. Kurita, and T. Tsuji, "Kansei-related assessment in a subjective force perception space and its application to a design for steering wheel operation characteristics," *Trans. Soc. Automotive Eng. Jpn.*, vol. 81, no. 822, 2015, Art. no. 014463.
- [15] L. A. Jones, "Perception of force and weight: Theory and research," *Psychol. Bull.*, vol. 100, no. 1, p. 29, 1986.
- [16] K. Takemura, N. Yamada, A. Kishi, K. Nishikawa, T. Nouzawa, C. Li, Y. Kurita, and T. Tsuji, "A subjective force perception model of humans and its application to a steering operation system of a vehicle," in *Proc. IEEE Int. Conf. Syst., Man, Cybern.*, Oct. 2013, pp. 3675–3680.
- [17] D. McCloskey, S. Gandevia, E. Potter, and J. Colebatch, "Muscle sense and effort: Motor commands and judgments about muscular contractions," *Adv. Neurol.*, vol. 39, pp. 151–167, Jan. 1983.
- [18] E. Cafarelli and B. Bigland-Ritchie, "Sensation of static force in muscles of different length," *Exp. Neurol.*, vol. 65, no. 3, pp. 511–525, Sep. 1979.
- [19] H. M. Morree, C. Klein, and S. M. Marcora, "Perception of effort reflects central motor command during movement execution," *Psychophysiology*, vol. 49, no. 9, pp. 1242–1253, Sep. 2012.
- [20] Y. Kishishita, K. Takemura, N. Yamada, T. Hara, A. Kishi, K. Nishikawa, T. Nouzawa, T. Tsuji, and Y. Kurita, "Prediction of perceived steering wheel operation force by muscle activity," *IEEE Trans. Haptics*, vol. 11, no. 4, pp. 590–598, Oct. 2018.
- [21] Y. Kishishita, Y. Tanaka, and Y. Kurita, "Force perceptual bias caused by muscle activity in unimanual steering," *PLoS ONE*, vol. 14, no. 10, Oct. 2019, Art. no. e0223930.
- [22] G. T. Fechner, *Elements of Psychophysics*, vol. 1. New York, NY, USA: Holt, Rinehart and Winston, 1966.
- [23] S. L. Delp, F. C. Anderson, A. S. Arnold, P. Loan, A. Habib, C. T. John, E. Guendelman, and D. G. Thelen, "OpenSim: Open-source software to create and analyze dynamic simulations of movement," *IEEE Trans. Biomed. Eng.*, vol. 54, no. 11, pp. 1940–1950, Nov. 2007.
- [24] A. Menegolo, *SimTK: Upper and Lower Body Model*. Accessed: Oct. 1, 2021. [Online]. Available: [https://simtk.org/projects/ulb\\_project](https://simtk.org/projects/ulb_project)
- [25] D. G. Thelen, "Adjustment of muscle mechanics model parameters to simulate dynamic contractions in older adults," *J. Biomech. Eng.*, vol. 125, no. 1, pp. 70–77, Feb. 2003.
- [26] K. R. S. Holzbaur, W. M. Murray, and S. L. Delp, "A model of the upper extremity for simulating musculoskeletal surgery and analyzing neuromuscular control," *Ann. Biomed. Eng.*, vol. 33, no. 6, pp. 829–840, Jun. 2005.
- [27] F. E. Zajac, "Muscle and tendon: Properties, models, scaling, and application to biomechanics and motor control," *Crit. Rev. Biomed. Eng.*, vol. 17, no. 4, pp. 359–411, 1989.
- [28] R. L. Lieber and S. C. Bodine-Fowler, "Skeletal muscle mechanics: Implications for rehabilitation," *Phys. Therapy*, vol. 73, no. 12, pp. 844–856, Dec. 1993.
- [29] C. Lanczos, *The Variational Principles of Mechanics*. Toronto, ON, Canada: Univ. of Toronto Press, 2020.
- [30] S. S. Stevens, "Problems and methods of psychophysics," *Psychol. Bull.*, vol. 55, no. 4, p. 177, Jul. 1958.
- [31] L. A. Jones and H. Z. Tan, "Application of psychophysical techniques to haptic research," *IEEE Trans. Haptics*, vol. 6, no. 3, pp. 268–284, Jul. 2013.
- [32] M. Emoto, K. Masaoka, M. Sugawara, and Y. Nojiri, "The viewing angle dependency in the presence of wide field image viewing and its relationship to the evaluation indices," *Displays*, vol. 27, no. 2, pp. 80–89, Mar. 2006.
- [33] J. Brooke, *System Usability Scale (SUS): A Quick-and-Dirty Method of System Evaluation User Information*, vol. 43. Reading, U.K.: Digital Equipment Co Ltd, 1986, pp. 1–7.
- [34] H. Sakoe and S. Chiba, "Dynamic programming algorithm optimization for spoken word recognition," *IEEE Trans. Acoust., Speech, Signal Process.*, vol. ASSP-26, no. 1, pp. 43–49, Feb. 1978.
- [35] F. Petitjean, A. Ketterlin, and P. Gançarski, "A global averaging method for dynamic time warping, with applications to clustering," *Pattern Recognit.*, vol. 44, no. 3, pp. 678–693, Mar. 2011.
- [36] S. Haga and N. Mizukami, "Japanese version of NASA task load index: Sensitivity of its workload score to difficulty of three different laboratory tasks," *Jpn. J. Ergonom.*, vol. 32, no. 2, pp. 71–79, 1996.
- [37] S. G. Hart and L. E. Staveland, "Development of NASA-TLX (task load index): Results of empirical and theoretical research," in *Advances in Psychology*, vol. 52. Amsterdam, The Netherlands: Elsevier, 1988, pp. 139–183.
- [38] C. Raima, M. Ito, S. Saiki, Y. Yamazaki, and Y. Kurita, "Developing a sense of agency scale for heavy machinery operation," in *Proc. 13th Int. Conf. Hum. Syst. Interact. (HSI)*, Jun. 2020, pp. 45–49.
- [39] S. Holm, "A simple sequentially rejective multiple test procedure," *Scand. J. Statist.*, vol. 6, pp. 65–70, Jan. 1979.
- [40] N. Hogan, "Adaptive control of mechanical impedance by coactivation of antagonist muscles," *IEEE Trans. Autom. Control*, vol. AC-29, no. 8, pp. 681–690, Aug. 1984.
- [41] R. Baratta, M. Solomonow, B. H. Zhou, D. Letson, R. Chuinard, and R. D'Ambrosia, "Muscular coactivation: The role of the antagonist musculature in maintaining knee stability," *Amer. J. Sports Med.*, vol. 16, no. 2, pp. 113–122, Mar. 1988.
- [42] P. L. Gribble, L. I. Mullin, N. Cothros, and A. Mattar, "Role of cocontraction in arm movement accuracy," *J. Neurophysiol.*, vol. 89, no. 5, pp. 2396–2405, May 2003.
- [43] R. Osu, D. W. Franklin, H. Kato, H. Gomi, K. Domen, T. Yoshioka, and M. Kawato, "Short- and long-term changes in joint co-contraction associated with motor learning as revealed from surface EMG," *J. Neurophysiol.*, vol. 88, no. 2, pp. 991–1004, Aug. 2002.
- [44] J. H. Mitchell, W. Haskell, P. Snell, and S. P. Van Camp, "Task force 8: Classification of sports," *J. Amer. College Cardiol.*, vol. 45, no. 8, pp. 1364–1367, Apr. 2005.
- [45] U. Proske and T. Allen, "The neural basis of the senses of effort, force and heaviness," *Exp. Brain Res.*, vol. 237, no. 3, pp. 589–599, Mar. 2019.
- [46] B. L. Luu, B. L. Day, J. D. Cole, and R. C. Fitzpatrick, "The fusimotor and reafferent origin of the sense of force and weight," *J. Physiol.*, vol. 589, no. 13, pp. 3135–3147, Jul. 2011.



- [47] J. Brooks, T. J. Allen, and U. Proske, "The senses of force and heaviness at the human elbow joint," *Exp. Brain Res.*, vol. 226, no. 4, pp. 617–629, May 2013.
- [48] D. Phillips, P. Kosek, and A. Karduna, "Force perception at the shoulder after a unilateral suprascapular nerve block," *Exp. Brain Res.*, vol. 237, no. 6, pp. 1581–1591, Jun. 2019.
- [49] F. Monjo, J. Shemmell, and N. Forestier, "The sensory origin of the sense of effort is context-dependent," *Exp. Brain Res.*, vol. 236, no. 7, pp. 1997–2008, Jul. 2018.
- [50] K. Higashi, S. Okamoto, and Y. Yamada, "Perceived hardness through actual and virtual damped natural vibrations," *IEEE Trans. Haptics*, vol. 11, no. 4, pp. 646–651, Oct. 2018.
- [51] H. Culbertson, J. M. Walker, M. Raitor, and A. M. Okamura, "WAVES: A wearable asymmetric vibration excitation system for presenting three-dimensional translation and rotation cues," in *Proc. CHI Conf. Hum. Factors Comput. Syst.*, May 2017, pp. 4972–4982.
- [52] S. B. Schorr and A. M. Okamura, "Three-dimensional skin deformation as force substitution: Wearable device design and performance during haptic exploration of virtual environments," *IEEE Trans. Haptics*, vol. 10, no. 3, pp. 418–430, Jul. 2017.
- [53] Z. F. Quek, W. R. Provancher, and A. M. Okamura, "Evaluation of skin deformation tactile feedback for teleoperated surgical tasks," *IEEE Trans. Haptics*, vol. 12, no. 2, pp. 102–113, Apr. 2019.
- [54] Y. Kamikawa, N. Enayati, and A. M. Okamura, "Magnified force sensory substitution for telemanipulation via force-controlled skin deformation," in *Proc. IEEE Int. Conf. Robot. Automat. (ICRA)*, May 2018, pp. 4142–4148.



**RYOTA SEKIZUKA** received the M.E. degree in engineering from Hiroshima University, Hiroshima, Japan, in 2019, where he is currently pursuing the Ph.D. degree with the Graduate School of Engineering.

He is a member of the Japan Society of Mechanical Engineers.



**MASARU ITO** received the M.E. degree in mechanical engineering from Kumamoto University, Kumamoto, Japan, in 2010, and the Ph.D. degree in human-machine interaction from Hiroshima University, Hiroshima, Japan, in 2021.

In 2010, he joined Kobelco Construction Machinery Company Ltd., Hiroshima. From 2017 to 2021, he was an Assistant Professor with the Next Generation Human Interface Collaborative Research Laboratory, Hiroshima University, where he was an Associate Professor, in 2021. He has been a Visiting Associate Professor with Hiroshima University, since 2021. His research interests include human interface, control engineering, and mechatronics.

Prof. Ito is a member of the Japan Society of Mechanical Engineers and the Society of Instrument and Control Engineers.



motor-skilled humans.

Prof. Raima is a member of the Japan Society of Mechanical Engineers.



**SEIJI SAIKI** joined Kobelco Construction Machinery Company Ltd., Hiroshima, Tokyo, Japan, in 2009, where he is currently the Manager of the DX Consulting Group, Business Development Department.



**YOICHIRO YAMAZAKI** received the M.E. degree in mechanical engineering from Ehime University, Ehime, Japan, in 1992.

From 1992 to 1999, he was with Kobe Steel, Ltd. Since 2019, he has been a Visiting Professor with Hiroshima University, Hiroshima. In 1999, he joined Kobelco Construction Machinery Company Ltd., Hiroshima, Tokyo, Japan, where he is currently the General Manager of the Business Development Department.

Prof. Yamazaki is a member of the Japan Society of Mechanical Engineers.



**YUICHI KURITA** (Member, IEEE) received the B.E. degree from Osaka University, in 2000, and the M.E. and Ph.D. degrees in information science from the Nara Institute of Science and Technology (NAIST), Japan, in 2002 and 2004, respectively.

From 2005 to 2007, he was a Research Associate with the Graduate School of Engineering, Hiroshima University, Japan. From 2007 to 2011, he was an Assistant Professor with the Graduate School of Information Science, NAIST. From 2010 to 2011, he was a Visiting Scholar with the School of Mechanical Engineering, Georgia Institute of Technology, Atlanta, GA, USA. Since 2011, he has been with the Graduate School of Engineering, Hiroshima University, as an Associate Professor, and a Professor, since 2018. He also works as an Assistant to President by special appointment and the Director of the Applied Human Augmentation Project Research Center, Hiroshima University. His research interests include human augmentation, haptics, and human-robot interaction.

Prof. Kurita is a member of the Japan Society of Mechanical Engineers, the Robotics Society of Japan, the Virtual Reality Society of Japan, and the Society of Instrument and Control Engineers.

...